ELSEVIER

Biophysical Chemistry 86 (2000) 221–230

Biophysical Chemistry

www.elsevier.nl/locate/bpc

Structural dynamics of myoglobin ☆

Maurizio Brunori*

Dipartimento di Scienze Biochimiche, Università di Roma 'La Sapienza', Piazzale Aldo Moro, 5, 00185 Roma, Italy

Received 27 January 2000; accepted 11 March 2000

Abstract

Conformational fluctuations have been invoked to explain the observation that the diffusion of small ligands through a protein is a global phenomenon, as suggested (for example) by the oxygen induced fluorescence quenching of buried tryptophans. In enzymes processing large substrates, a channel to the catalytic site is often seen in the crystal structure; on the other hand in small globular proteins, it is not known if the cavities identified in the interior space are important in controlling their function by defining specific pathways in the diffusion to the active site. This point is addressed in this paper, which reports some relevant results obtained on myoglobin, the hydrogen atom of molecular biology. Protein conformational relaxations have been extensively investigated with myoglobin because the photosensivity of the adduct with CO, O_2 and NO allows us to follow events related to the migration of the ligand through the matrix. Results obtained by laser photolysis, molecular dynamics simulations, X-ray diffraction of intermediate states of wt type and mutant myoglobins are briefly summarized. Crystallographic data on the photochemical intermediate of a new triple mutant of sperm whale myoglobin (Mb-YQR) show, for the first time, the photolyzed CO* sitting in one of the Xe-binding cavities, removed from the heme group. These results support the viewpoint that pre-existing 'packing defects' in the protein interior play a major role in controlling the dynamics of ligand binding, including oxygen, and thereby acquire a survival value.

Keywords: Cavities; Photolysis; Crystallography; Intermediates; Function

1. Packing defects and protein dynamics

Ever since the three-dimensional structure of lysozyme was solved [1], enzymes are often characterized by a cleft at the active site to host the substrate. In enzymes processing larger substrates, a channel guiding to the active site has been identified, and the molecular basis of substrate channeling is now understood [2].

In small globular proteins, 'packing defects' identified in the interior space as void volumes [3] are essential structural components of protein flexibility and thermodynamic stability. The common observation that many thermophilic proteins are more stable and more rigid than their meso-

☆ This paper is a tribute to my dear friend Heini Eisenberg (Rehovot, Israel)

* Tel.: +39-06-4450291; fax: +39-06-4440062.
E-mail address: brunori@axrma.uniroma1.it (M. Brunori).

0301-4622/00/$ - see front matter
PII: S0301-4622(00)00142-3

philic counterparts has been considered as the basis for their lower reaction rates at room temperature [4].

How important internal cavities are in functional control, by providing pathways and hosting stations in the diffusion of a ligand to the active site, remains an open problem. The concept that protein fluctuations and conformational changes are linked to structural defects was defined by Lumry [5] as the 'mobile defect hypothesis'. Ever since, this idea gained support, although it seems now clear that defects are well-defined cavities, which may or may not mediate ligand migration in proteins. This paper is about finding the functional value of these internal 'packing defects', based on recent crystallographic data [6] of a novel photochemical intermediate of a triple mutant of myoglobin (Mb).

2. Myoglobin

Mb is a small globular protein whose function in the red muscles is to facilitate O_2 delivery to the mitochondrion. O_2 is bound to the ferrous (Fe II) heme with an overall dissociation constant ($K_D \sim 1$ μM) intermediate between that of mitochondrial cytochrome-*c*-oxidase ($K_M < 0.1$ μM) and that of hemoglobin in the erythrocyte ($K_D \sim 25$ μM). The ferrous state of Mb binds CO and NO with affinities higher than that for O_2 [7].

The model of the active site of sperm whale Mb is shown in Fig. 1 as a complex with O_2, CO and NO. Only some of the amino acid side chains surrounding the heme are highlighted; in particular those on the distal site, which are in close contact with the iron bound ligand and play a role in the discrimination between these three gases, which bind with very different affinities and rates (see [7] and [10] for reviews). Examination of a space-filling model shows that there is no clear channel that these diatomic molecules may follow to come in close contact with the heme iron [11], and fluctuations of the side chains should open a passageway for the ligand to diffuse to and from the active site.

Molecular dynamic (MD) simulations of Mb (and of the hemoglobin chains) provided information on the motions of the iron and the protein, and on the escape of the ligand from the active site [12,13]. An initial hypothesis for ligand migration from the heme into the solvent was based on the so-called His-gate, which involves a rotation of the side chain of the distal His 64 (E7) to create a channel [14]. Experimental evidence in favor of this mechanism includes a displacement of His 64 (E7), as seen in the crystal structure of some derivatives [15,16], as well as large changes in the rate constants for ligand entry in Mb mutants [17]. MD simulations [18] and random mutagenesis data [19] indicated alternative pathways for ligand escape, involving hydrophobic residues between the B, G and H helices.

A special feature which makes hemoproteins ideal objects to study the rapid migration of a ligand in the matrix, is the photosensivity of the Fe-ligand bond [7]. Since Gibson's discovery of the quickly reacting state of hemoglobin [20], tremendous progress has been achieved. The advent of super-fast lasers opened new avenues to study the relaxation of the protein and the migration of the ligand in a time range extending from picoseconds-to-microseconds. In this field, the conceptual breakthrough came with the discovery of geminate recombination and the role of conformational substates of a protein on its function [21].

3. Kinetic barriers to ligand binding

The kinetics of ligand re-binding to Mb has been extensively investigated by laser spectroscopy, because of the photosensivity of the adduct with O_2, CO, NO, and other ferrous ligands [7]. These diatomic molecules are small enough to allow rapid migration away from the metal, and large enough to probe the accessibility of atomic size cavities in the protein's interior. The high photosensivity of the Mb–CO adduct has made this complex ideal for early photochemical work on hemoglobin; on the other hand O_2 and NO, because of their higher intrinsic reactivity, have proved to be very useful probes of the earlier events, after picosecond-to-nanosecond laser dissociation.

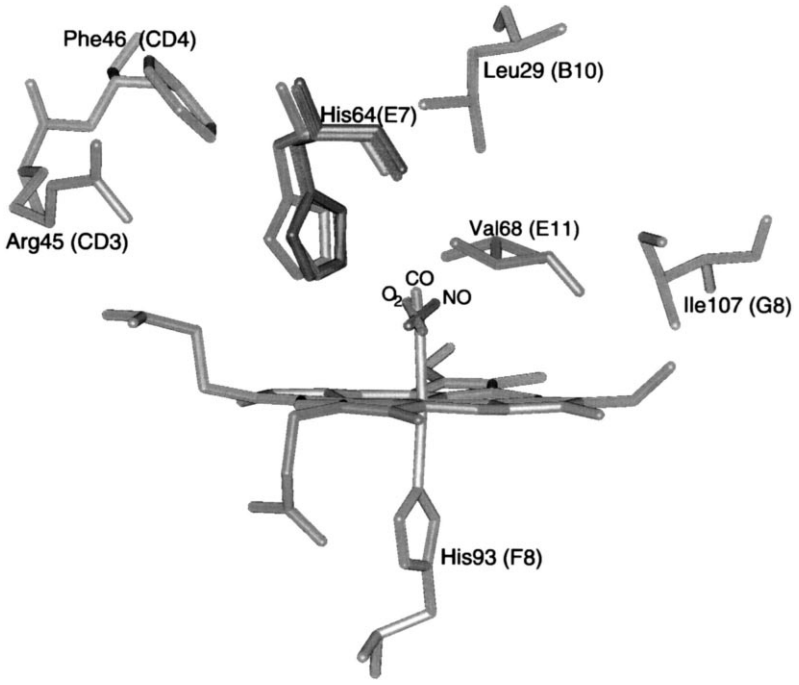

Fig. 1. View of the distal pocket of Mb bound to O_2, NO, and CO. Coordinates from Quillin et al. [8] for MbO_2 (2 mhm) and for MbCO (2 mgk), and Brucker et al. [9] for MbNO (1 hjt). A number of amino acid side chains, which are important in controlling dynamics and the affinity of ligand binding, are indicated. The position of His 64 (E7) is at a distance suitable to interact with the bound ligand. Notice that O_2 and NO have a bent geometry (111–120° for O_2 and 111–140° for NO), while CO is more linear (155–180°). The H-bond with His 64 (E7) which stabilizes O_2, is much weaker with NO and essentially absent with CO.

Optical spectroscopy of ligand binding after the rapid photodissociation of MbCO led to the discovery of the geminate state [21,22]. The rupture of the Fe–CO bond by an intense light pulse leads to an immediate change in the spectrum of Mb; the photolyzed ligand can either migrate out into the solvent (and thereby re-bind in a slow bimolecular mode), or hit the iron diffusing from within the protein; an intramolecular process called geminate recombination. The presence of at least one intermediate state suggested a simple two-step reaction scheme [23], illustrated by the free energy barrier diagram reported in Fig. 2. Examination of the diagram shows that the outer barrier (~ 4 kcal mol^{-1}) is related to the diffusion in the interior of the protein, and is essentially the same for the three ligands. The inner barrier, which leads to the bound state, has a very different height for the three gases, and reflects differences in intrinsic reactivity. It should not be forgotten that the bound ligands have a different stereochemistry, as shown in Fig. 1. The mechanism of discrimination by the protein moiety has been extensively investigated [10].

Because of quantum mechanical restrictions, geminate rebinding of CO to Mb at room temperature is minimal and thus it has been very difficult to detect; only very accurate spectroscopic data [24] provided unequivocal evidence for the nanosecond rebinding of CO to Mb. O_2 is more reactive, and on a nanosecond time scale yields approximately 50% geminate rebinding in Mb; thus it has been extensively employed with a number of mutants, not only because it is the physiological ligand, but in order to evaluate ligand migration. The highest reactivity by far is seen with NO, which rebinds to Mb almost completely in a time scale of picoseconds, because of

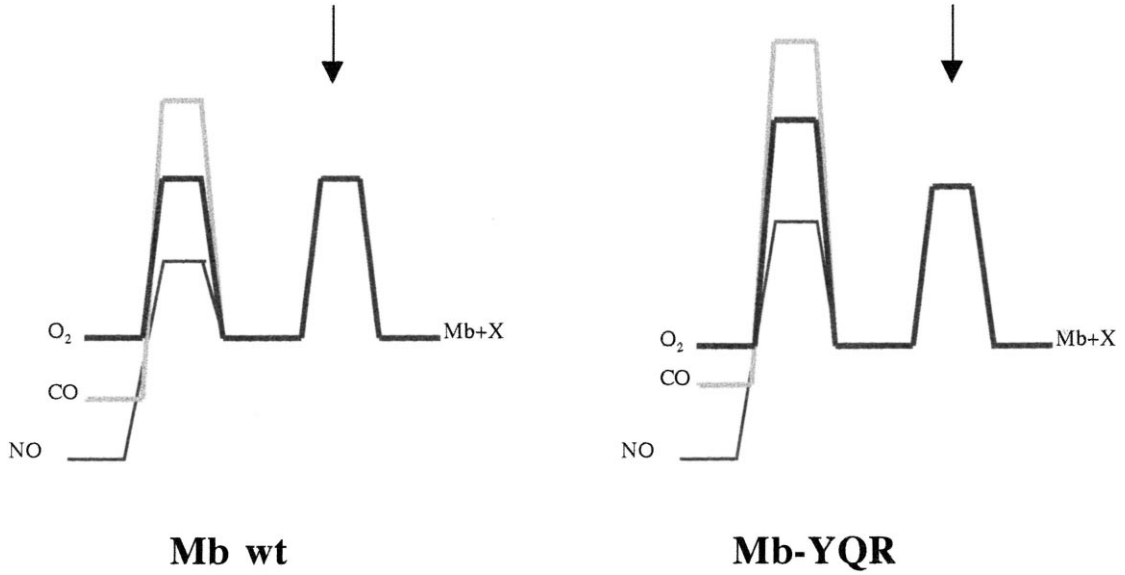

Fig. 2. Free energy barrier diagram for the binding of O_2, CO and NO to wt Mb (left) and to Mb-YQR (right). From Brunori et al. [38], modified. The solution state (S = Mb + X) is arbitrarily set to free energy = 0. The outer barrier (arrow) is essentially the same for the three ligands and the two Mbs ($\sim$ 4 kcal mol^{-1}). The inner barrier is different; for wt Mb, the inner barrier is small for NO, approximately equal to the outer barrier for O_2, and much larger for CO. In general, mutations of the distal site residues affect the inner barrier (see Olson and Phillips [23] for a review). Thus mutations introduced in Mb-YQR lead to a substantial decrease of the overall combination rate constants for O_2 and CO because binding demands the concerted fluctuation of Tyr 29 (B10) and Gln 64 (E7) that in the deoxygenated protein move towards the heme and hinder close approach to the metal.

little quantum mechanical barrier. The multiphasic nature of NO geminate rebinding [25,26] has been an important probe to assess the role of the protein in the control of ligand binding.

The kinetics and the yield of the geminate phase are both sensitive to the local conformation of the heme, and, therefore, to its immediate environment (Fig. 1). The role of the protein is crucial to control reactivity and function, and thus it was proposed that the kinetic barrier for ligand rebinding is controlled by the protein; the exact origin of this control has been extensively investigated [25–30]. It may be recalled that the multiphasic rebinding may be determined by: (i) the relaxation of the Fe–His 93 (F8) bond ('proximal effect'), with the metal moving out of the heme plane after ligand dissociation, and thereby slowing-down geminate rebinding; or (ii) the migration of the photolyzed ligand in the matrix, with rebinding by diffusion from sites at various distances from the heme iron.

The conformational relaxation of the protein after instantaneous photodissociation covers a large time interval, and has been described with a continuous distribution of exponential processes (see [30,31,32]). Important features emerged from a complete study of the protein relaxation as a function of temperature and viscosity in Mb and Hb [31,33]. The origin of the stretched exponential kinetics in the higher temperature range led to the proposal of different models which emphasize either the difference in the well depth for the various conformational substates [34], or the change in the distribution of solvated slowly interconverting molecules [33]. Ansari et al. [31] concluded that at very low temperatures, the conformational substates of Mb are not so much 'frozen' but 'stuck', emphasizing the effect of viscosity and internal diffusion.

A consecutive reaction scheme involving (at least) four states has been commonly employed, as illustrated in the following Eq.(1):

$$\underset{A}{MbX} \Leftrightarrow \underset{B(ps)}{Mb{:}X^*} \Leftrightarrow \underset{C(ns)}{Mb{::}X^*} \Leftrightarrow \underset{S(ms)}{Mb + X} \quad (1)$$

In the discussion of this scheme with reference to the role of 'packing defects' on function, we take into consideration the viewpoint championed by Gibson and collaborators [23,25,29], that multiphasic geminate rebinding is primarily determined by the migration of the ligand away into the matrix. However, the alternative hypothesis, that the relaxation of the Fe out of the heme plane ('proximal effect') plays a role, should not be forgotten [28,30,33].

Photochemical or thermal dissociation of MbX is associated with the rapid motion of X* (the ligand in the matrix) into the distal pocket, shown in Fig. 1. The ligand reaches a primary docking site (B-state) in less than 1 ps, and CO* acquires two orientations which are both parallel to the heme plane [35]. Lim et al. interpreted their time resolved IR data to mean that in the B-state (Mb:X*) the CO* is trapped by the protein fairly close to the metal. The location may be the same, accounting for the very fast NO geminate rebinding phase, because of back diffusion from a relatively close position hitting the iron. A role for the side chain of Leu 29 (B10) has been established by site-directed mutagenesis; with Phe in (B10), most of the ligand dissociated by the light pulse is bounced back to increase the probability of contact with the iron, and rebinding with NO is extremely fast (see Olson and Phillips [23]). If rebinding is made difficult by quantum mechanical restrictions, the ligand migrates away and eventually reaches the solvent (S-state); this is generally the destiny for CO* because the inner barrier exceeds by far the outer barrier (see Fig. 2).

Much debate has gone into the interpretation of the C-state(s), associated with the picosecond-to-nanosecond rebinding phase (0.5–500 ns). A common view is that the C-state is correlated to the trapping of the ligand into new and more distant locations, called secondary docking sites [36]. Some of the results on site-directed mutants of Mb seem consistent with this hypothesis (see Olson and Phillips [23]). We studied a triple mutant of Mb (designed to mimic the O_2 binding properties of Ascaris Hb (see [37]) which is characterized by a very slow ($\tau \sim 200$ ns) and prominent geminate phase with NO, and an unusually large μs quantum yield ($\sim 4\%$) [38]. Based on MD simulations, and on the effect of Xe on the time course of geminate NO rebinding, it was proposed [38] that a fraction of NO* migrates into a cavity which corresponds to the Xe^4 site of Tilton et al. [39]. Since this behavior was observed with NO which has the highest intrinsic reactivity, the simple-minded view that the ligand was trapped further away (> 8 Å) into a secondary docking site seemed logical. Nonetheless these data will have to be reconciled with the view held by Olson and Phillips [23], who argued that, even for the ns geminate phase, the ligand is close to the iron but distributed among a smear of positions.

The uncertainties in the exact location and nature of these secondary docking sites poses a number of problems which may be relevant to the pathway of ligand entry in the molecule. The overall rebinding rate demands a close approach to the iron. In wt Mb, binding is possible after the expulsion of a water molecule stabilized near the metal by H-bonding to His 64 (E7) [40]. In several mutants, a reduction of the space in the distal pocket by the insertion of bulky residues decreases the overall second order rate constant. Examples are the Val 68 (E11) → Phe and the Leu 29 (B10) → Tyr mutants; on the other hand smaller residues as in Leu 29 (B10) → Ala have opposite effects (see [23]). The correlation of this extensive kinetic information with the location of cavities and their connectivity is dealt with in the following paragraph.

4. Cavities and pathways

Xenon proved to be a useful probe to study the number and location of 'packing defects' in met-Mb [39]. The X-ray crystallographic data at 1.9 Å resolution revealed four binding sites with an occupancy from 0.45 to 1.0. These cavities (called Xe^1 through to Xe^4) have radii greater than 1.2 Å, are coated largely by hydrophobic residues (Leu, Ile, Val, Phe) and exist within the globin

structure even in the absence of Xe, since they can be filled with minimal perturbation and (if anything) a decrease in local atomic motions. The location of the four Xe atoms is shown in Fig. 3. Xe^1 and Xe^2 are relatively close to the Fe and to each other on the proximal side of the heme; some of the residues defining this cavity are Leu 89, Ala 90, His 93, Leu 104, Phe 138 and Ile 142. Xe^3 resides in a cavity near the surface, screened from the solvent by Ala 134 and Gly 80, and far (13.5 Å) from the iron. Xe^4 is on the opposite side of the heme, in a space bounded by the residues Gly 25, Ile 28, Leu 29, Val 68, and Ile 107. This pioneering work yielded a static picture of a few cavities, occupied by Xe with different 'affinities', and pre-existing in the globin's interior. However, it provided no information on the movement of small ligands in the matrix and on the possible role of 'packing defects' on the rates of ligand binding to Mb.

Molecular dynamics (MD) simulations carried out by Karplus, Elber and co-workers [18,41], led to the identification of multiple pathways for the escape of CO from Mb. The enhanced sampling algorithm follows the motion of a cloud of 60 ligand molecules in the presence of a single trajectory of the protein. Ligands were found to be trapped for significant times in individual cavities, which corresponded to the Xe binding sites; hopping between cavities and/or escape to the solvent were rare and rapid events, involving the crossing of barriers. Escape from the protein was through several routes, but most of the trajectories passed near the heme, Ile 107 (G8) and Val 68 (E11) (shown in Fig. 1). In all events, computations confirmed that rapid protein fluctuations are essential for the escape of small diatomic molecules from the matrix into the solvent.

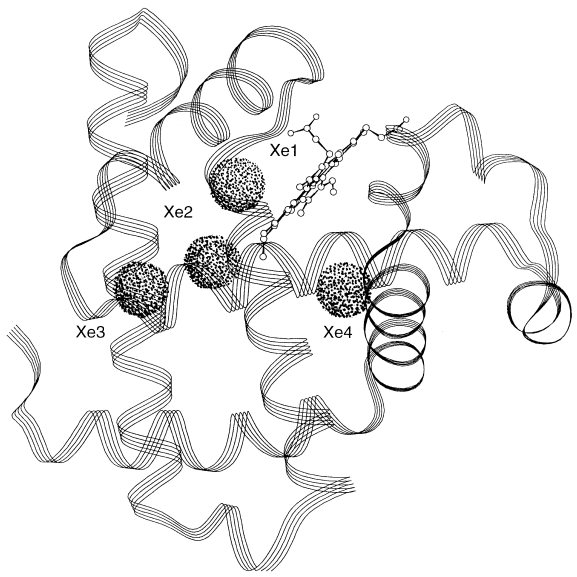

Fig. 3. Crystallographic structure at 1.9 Å resolution of sperm whale met-Mb under Xe gas at 7 atm. From Tilton et al. [39], modified. The four Xe atoms bound are shown as dotted spheres, and the protein backbone as a ribbon; the heme is seen edge-on, with the proximal site toward the upper left.

Multiple ligand escape pathways were probed by an original approach introduced by Huang and Boxer [19]. A random library of single base mutations of the Mb gene was generated, and the colonies expressing Mb were probed by laser photolysis of crude lysates of *E. coli*. Examination of approximately 1500 mutant Mbs led to the discovery that a large fraction (10%) exhibited major differences in the time course of the ligand (O_2 and CO) rebinding compared to the wt protein. Mutated residues, associated with a measurable kinetic effect, tend to occur as clusters in the three-dimensional structure; the authors described nine possible clusters, some corresponding to the residues involved in defining the Xe-binding cavities [39].

A revealing piece of work by Scott and Gibson [36] made the important step of correlating the Xe binding cavities and pathways to ligand rebinding and escape in sperm whale Mb mutants. These authors reported geminate O_2 rebinding data (from ns to μs) on more than 25 point mutants, in the absence and presence of Xe. The time course of this reaction is biphasic. The initial fast phase (half time $\sim$20 ns) is larger in amplitude, and is accelerated in the presence of Xe; the slower phase (half time $\sim$0.5–2.0 μs) is smaller in amplitude and is affected by a number of point mutations and by a high pressure of Xe gas. The authors describe their data with a side-path model, whereby the photodissociated ligand

moves initially into a primary docking site toward the interior of the protein, and upwards to a position in the direction of Leu 29 (B10), Ile 107 (G8) and the Xe^4 site (see above), in the initial picoseconds after dissociation [35]. From the primary docking site the ligand may: (i) diffuse back to the Fe and rebind; (ii) escape on the opposite side (possibly through the His–gate); or (iii) migrate to the Xe^4 and/or to the Xe^1 sites. From these secondary docking sites, ligands may diffuse back, accounting for the slower O_2 geminate phase. The effect of Xe (at different pressures up to 12 atm) and of single mutations on the rate parameters of the side-path model, and on the amplitude of the secondary phase, allows us to map the secondary docking sites. Particularly significant effects were obtained with mutants of Leu 29 (B10) (to Ala or Trp) and mutants of Leu 104 (G5) (to Ala and Trp again). In particular, the mutation Leu 104 (G5) → Trp behaves as though the aromatic side chain occupies the Xe^1 site (and possibly close to the Xe^2 site, see above).

This study made the necessary connection between the crystallographic data locating the Xe binding sites, the MD calculations, and the kinetics of ligand rebinding from different locations in the protein matrix. Within the limitations of the side-path model (and without necessarily proving that the sequential model, see Eq. (1), is inapplicable), Scott and Gibson [36] presented a coherent correlation between the location of the ligand within the protein and the speed of the geminate rebinding to the Fe, concluding that the slower geminate phase reflects the migration of the ligand towards the metal from secondary docking sites, corresponding to the Xe^1, Xe^2, and Xe^4 of Tilton et al. [39]. Crystallographic data on the photolytic intermediates are described below in connection with these kinetic experiments.

5. The structure of photochemical intermediates

The first attempt to correlate crystallographic information with the dynamic behavior of Mb can be traced back to Frauenfelder et al., [42] who reported the temperature dependence of the protein fluctuations evaluated from B-factor analysis. The last few years have seen the first successful attempts to determine directly the structure of photochemical intermediate(s) obtained by the photolysis of CO bound to ferrous Mb in single crystals.

The first time-resolved X-ray diffraction experiment [43] with ns time resolution, revealed a number of features related to the position of the photodissociated CO* and the motion of the Fe and of the protein. Together with previous work at ultra-low temperatures [44–46], the diffraction data at room temperature showed the CO* to be located in a site fairly close to the Fe, which moves out of the heme plane (by ~ 0.3 Å) with a concerted motion of the proximal His 93 (F8). In spite of some differences in yield and location, attributed (partially or totally) to a variable degree of photolysis related to the experimental protocol and/or the temperature [46], the results showed that CO* is a few Å from the metal, and probably in a position reached a few picoseconds after photolysis [35]. We can assume that this primary docking site corresponds to the location that leads to the faster geminate O_2 rebinding [36].

A more extensive study of the structure of intermediates of Mb by crystallography of time resolved or 'frozen' species is of general interest. If the niche hosting the photolyzed CO* can be defined as a specific docking site, a correlation between the cavities where Xe is bound and the location of CO* may be expected. Since mutations were found to affect the time course of geminate rebinding, it may be anticipated that suitable mutants may result in a modification of the cavity occupied by the ligand during fast migration in the protein matrix, and thus protein engineering may be used to modify the preferential pathways. A crystallographic experiment reported by Brunori et al. [6], on a novel mutant of Mb, seems to provide relevant results.

The triple mutant of sperm whale Mb called Mb-YQR [37], contained the following mutations: Leu 29 (B10) → Tyr; His 64 (E7) → Gln; Thr 67 (E10) → Arg. An investigation using crystallography, kinetics and MD simulations [38] suggested that in Mb-YQR the photodissociated NO* migrates into a secondary docking site at some dis-

tance from the Fe. The effect of Xe on the time course of geminate recombination and MD simulations suggested that this may correspond to the Xe^4 site of Tilton et al. [39]. In this work NO was employed because of its higher intrinsic reactivity, associated with large nanosecond geminate phases, but the behavior of CO and O_2 was also studied. This investigation is fully consistent with the view held by Gibson and co-workers [25,29,36], that the origin of multiphasic geminate reactions is not related to the movement of the Fe out of the heme plane after photodissociation, but to diffusion of the photolyzed ligand away from the metal, partially into more distant sites.

The structure of the photolytic intermediate of Mb-YQR was determined at 20 K by X-ray diffraction, following the protocol of Schlichting et al. [44]. Starting with the CO complex of Mb-YQR, illumination and photolysis of the Fe–CO bond is associated with the migration of CO* to a cavity 8.1 Å away from the metal [6] (see Fig. 4), which corresponds to that predicted by MD simulations. The photolytic intermediate undergoes small structural changes in the protein. On the proximal side, the Fe and His 93 (F8) move away from the heme plane as in the wt protein; on the distal side, motion of Tyr 29 (B10) and Gln 64 (E7), seen upon deoxygenation at room temperature [38], is very small at 20 K.

This secondary docking site becomes accessible to the ligand via a channel going by Ile 107 (G8), identified by Elber and Karplus [18,41], along a major escape route for CO*. This residue was found to be influential in geminate kinetic experiments carried out on single site mutants [36]. Brunori et al. [6] proposed that the mutations introduced in Mb-YQR dictate the preferential docking site occupied by the dissociated CO*. The mutation Leu 29 (B10) → Tyr seems sufficient, as illustrated in Fig. 4, to account for the differences seen between wt Mb and Mb-YQR. This interpretation supports the view that small ligands migrate to and from the active site through a limited number of voids and channels, which can be engineered. Moreover, this finding agrees with the proposal that there is a correlation between geminate rebinding kinetics and the location of the ligand into specific sites in the matrix.

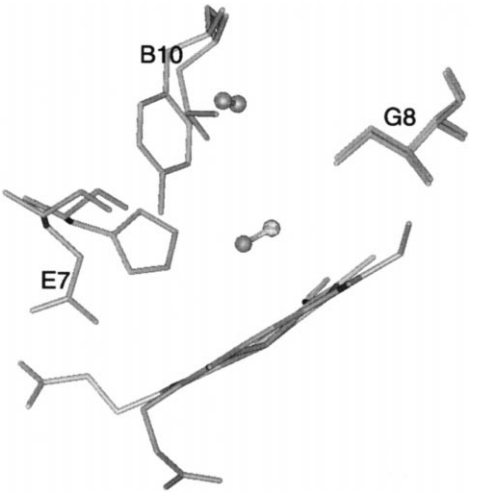

Fig. 4. Structure of the active site of Mb for the photochemical intermediate of the wt protein and the mutant Mb-YQR. Data from Schlichting et al. [44] and Brunori et al. [6]. The figure shows the heme edge-on, and three side chains on the distal site, namely: (E7) which is His in wt Mb and Gln in Mb-YQR; (B10) which is Leu in wt Mb and Tyr in Mb-YQR; and (G8) which is Ile in both. The position of the photolyzed CO* in the intermediate, as obtained by the rupture of the Fe–CO bond (diffraction data at 20 K), is indicated: (i) in the primary docking site as populated in wt Mb (near the heme), and (ii) in the secondary docking site as populated in Mb-YQR (shown near B10). Substitution of Leu 29 (B10) with Tyr seems sufficient to account for the observation that the preferential docking site of CO* in the two proteins is different and (by-and-large) alternative. The position of CO* in the primary docking site seems incompatible with Tyr at 29 (B10) since its hydroxyl would be only 2.8 Å away from CO*; this may account for the very low occupancy of CO* in the primary docking site in the photolytic intermediate of Mb-YQR. On the other hand, Leu 29 (B10) in wt Mb would clash with CO* if this were to occupy the secondary docking site, being only 2.4 Å away from it; thus this niche, which hosts Xe^4, is less available for CO* in wt Mb.

Recent work by Parak et al. [47] seems to complete the picture just outlined, by using another Mb mutant of the same amino acid, namely Leu 29 (B10) → Trp. In these crystallographic experiments, the location of the photolyzed CO* depends on the protocol. When data were collected at 105 K after photolysis was carried out below 180 K, there was a complete dissociation

and the CO* was found in the back of the distal pocket, with minor displacements of the distal side chains. However, if photolysis was carried out above 180 K (and data were collected again at 105 K), large shifts of the side chains, especially His 64 (E7) and Trp 29 (B10) were seen; CO* was now located on the proximal side of the heme, in the Xe^1 (and Xe^2?) sites, with a 62% occupancy.

These crystallographic data on the photolytic intermediates of mutant Mbs agree with the O_2 geminate recombination experiments [36] showing that, over and above the primary docking site yielding faster geminate rebinding, two secondary docking sites corresponding to Xe^4 and Xe^1 binding cavities can be occupied. Thus, a correlation between cavities, distance from the heme and kinetics of binding is supported.

6. Concluding remarks

In this paper, I have discussed the hypothesis that Mb internal cavities and 'packing defects' define a pathway for ligand diffusion to and from the active site, which is deeply buried inside the protein. Some of the results, obtained by crystallography of equilibrium and intermediate states of wt and mutant Mb, have been correlated with laser photolysis experiments (covering events in the picosecond-to-nanosecond time range) and MD simulations in order to present a coherent summary of the structural dynamics of Mb. Although oversimplified, the view presented leads to the general conclusion that cavities are specific docking sites and hosting stations, which play a role in controlling the dynamics of ligand binding and which can be modified by protein engineering. The emerging picture is that the migration of small diatomic molecules occurs through a limited number of docking sites, which in the case of Mb, have been identified largely with two of the Xe binding sites. The effect of filling these 'packing defects' with Xe at high pressure was a key observation to correlate cavities and function.

Overall binding rates and affinities have been described with a mechanism involving multiple states and barriers. Since some of the intermediates should correspond to Mb molecules with the ligand sitting in one or the other of the identified docking sites, en route to and from the iron, and given that the thermally dissociated ligand should follow the same pathway and cross the barriers estimated from photochemistry, a relevant question arises as to whether internal cavities and rapid fluctuations of side chains confer a selective advantage for survival. We have previously raised this point with reference to a specific comparison between two non-cooperative hemeproteins, suggesting that there may be an evolutionary value in internal protein dynamics, which may be involved in regulating O_2 rates and affinities [48]. Whether the specific case in question will stand the test of new experiments remains to be seen. Nevertheless, the general concept of a functional role of internal cavities (as anticipated with the 'mobile defect hypothesis') is complementary to the view that flexibility and stability in proteins are also related to cavities. Thus, there may be a selective advantage in building a protein with 'packing defects'.

Acknowledgements

Work supported by A.S.I. and by M.U.R.S.T. (PRIN 'Biologia Strutturale' 1999 to M.B.) The author is grateful to Prof. D. Tsernoglou for his crucial role in establishing the Protein Crystallography Unit at the University of Roma 'La Sapienza', and to Drs A. Bellelli, F. Cutruzzolà, A.E. Miele, C. Travaglini-Allocatelli and B. Vallone for their long-standing invaluable collaboration.

References

[1] D.C. Phillips, Sci. Am. 215 (1966) 78.
[2] E.W. Miles, S. Rhee, D.R. Davies, J. Biol. Chem. 274 (1999) 12193.
[3] F.M. Richards, Annu. Rev. Biophys. Bioeng. 6 (1977) 151.
[4] P. Zavodsky, J. Kardos, A. Svingor, G.A. Petsko, Proc. Natl. Acad. Sci. USA 95 (1998) 7406.
[5] R. Lumry, A. Rosenberg, Colloq. Int. CNRS 246 (1975) 53.

[6] M. Brunori, B. Vallone, F. Cutruzzolà, C. Travaglini-Allocatelli, J. Berendzen, K. Chu, RM. Sweet, I. Schlichting, Proc. Natl. Acad. Sci. USA 97 (2000) 2058.
[7] E. Antonini, M. Brunori, Hemoglobin and Myoglobin in their Reactions with Ligands, North Holland, Amsterdam, 1971.
[8] M.L. Quillin, R.M. Arduini, J.S. Olson, G.N. Phillips, J. Mol. Biol. 234 (1993) 140.
[9] E.A. Brucker, J.S. Olson, M. Ikeda-Saito, G.N. Phillips, Proteins 30 (1998) 352.
[10] B.A. Springer, S.G. Sligar, J.S. Olson, G.N. Phillips, Chem. Rev. 94 (1994) 699.
[11] M.F. Perutz, F.S. Mathews, J. Mol. Biol. 21 (1965) 199.
[12] D.A. Case, M. Karplus, J. Mol. Biol. 132 (1979) 343.
[13] E.R. Henry, M. Levitt, W.A. Eaton, Proc. Natl. Acad. Sci. USA 82 (1985) 2034.
[14] M.F. Perutz, Trends Biochem. Sci. 14 (1989) 42.
[15] M. Bolognesi, E. Cannillo, P. Ascenzi, G.M. Giacometti, A.M. Merli, A. Coda, M. Brunori, J. Mol. Biol. 158 (1982) 305.
[16] D. Ringe, G.A. Petsko, D. Kerr, P.R. Oritz de Montellano, Biochemistry 23 (1984) 2.
[17] H.H. Lai, T. Li, D.S. Lyons, G.N. Phillips, J.S. Olson, Protein Struct. Funct. Genet. 22 (1995) 322.
[18] R. Elber, M. Karplus, J. Am. Chem. Soc. 112 (1990) 9161.
[19] X. Huang, S.G. Boxer, Nature Struct. Biol. 1 (1994) 226.
[20] Q.H. Gibson, Biochem. J. 71 (1959) 293.
[21] R.H. Austin, K.W. Beeson, L. Eisenstein, H. Frauenfelder, I.C. Gunsalus, Biochemistry 14 (1975) 5355.
[22] H. Frauenfelder, F. Parak, R.D. Young, Annu. Rev. Biophys. Biophys. Chem. 17 (1988) 451.
[23] J.S. Oslon, G.N. Phillips, J. Biol. Chem. 271 (1996) 17593.
[24] E.R. Henry, J.H. Sommer, J. Hofrichter, W.A. Eaton, J. Mol. Biol. 166 (1983) 443.
[25] Q.H. Gibson, R. Regan, R.R. Elber, J.S. Olson, T.E. Carver, J. Biol. Chem. 267 (1992) 22022.
[26] K.A. Jogeward, D. Magde, D.J. Taube, I.C. Marsters, T.G. Traylor, V.S. Sharma, J. Am. Chem. Soc. 110 (1988) 380.
[27] J.M. Friedman, Science 228 (1985) 1273.
[28] J.W. Petrich, J.C. Lambry, K. Kuczera, M. Karplus, C. Poyart, J.L. Martin, Biochemistry 30 (1991) 3975.
[29] M. Ikeda-Saito, Y. Dou, T. Yonetani, J.S. Olson, T. Li, R. Regan, Q.H. Gibson, J. Biol. Chem. 268 (1993) 6855.
[30] J.M. Friedman, Methods Enzymol. 232 (1994) 205.
[31] A. Ansari, C.M. Jones, E.R. Henry, J. Hofrichter, W.A. Eaton, Biochemistry 33 (1994) 5128.
[32] M. Lim, T.A. Jackson, P.A. Anfirud, Proc. Natl. Acad. Sci. USA 90 (1993) 5801.
[33] J. Huang, A. Ridsdale, J. Wang, J.M. Friedman, Biochemistry 36 (1997) 14353.
[34] S.J. Hagen, W.A. Eaton, J. Chem. Phys. 104 (1996) 3395.
[35] M. Lim, T.A. Jackson, P.A. Anfirud, Nature Struct. Biol. 4 (1997) 209.
[36] E.E. Scott, Q.H. Gibson, Biochemistry 36 (1997) 11909.
[37] C. Travaglini-Allocatelli, F. Cutruzzolà, A. Brancaccio, B. Vallone, M. Brunori, FEBS Lett. 352 (1994) 63.
[38] M. Brunori, F. Cutruzzolà, C. Savino, C. Travaglini-Allocatelli, B. Vallone, Q.H. Gibson, Biophys. J. 76 (1999) 1259.
[39] R.F. Tilton, I.D. Kuntz, G.A. Petsko, Biochemistry 23 (1984) 2849.
[40] T.E. Carver, R.J. Rohlfs, J.S. Olson, Q.H. Gibson, R.S. Blackmore, B.A. Springer, S.G. Sligar, J. Biol. Chem. 265 (1990) 20007.
[41] R. Elber, A. Roitberg, C. Simmerling, R. Goldstein, H. Li, G. Verkhiver, C. Keaser, J. Zhang, A. Ulitsky, Comput. Phys. Comm. 91 (1995) 159.
[42] H. Frauenfelder, G.A. Petsko, D. Tsernoglou, Nature 280 (1979) 558.
[43] V. Srajer, T.Y. Teng, T. Ursby, C. Pradervand, Z. Ren, S. Adachi, W. Schildkamp, D. Burgeois, M. Wulff, K. Moffat, Science 274 (1996) 1726.
[44] I. Schlichting, J. Berendzen, G.N. Phillips, R.M. Sweet, Nature 371 (1994) 808.
[45] T.Y. Teng, V. Srajer, K. Moffat, Nature Struct. Biol. 1 (1994) 701.
[46] H. Hartman, S. Zinser, P. Komnions, R.T. Schneider, G.U. Nienhaus, F. Parak, Proc. Natl. Acad. Sci. USA 93 (1996) 7013.
[47] A. Ostermann, R. Waschipky, FG. Parak, GU. Nienhaus, Nature. 404 (2000) 205.
[48] M. Brunori, F. Cutruzzolà, C. Savino, C. Travaglini-Allocatelli, B. Vallone, Q.H. Gibson, Trends Biochem. Sci. 24 (1999) 253.